Lab-on-fiber optofluidic platform for in situ monitoring of drug release from therapeutic eluting polyelectrolyte multilayers

Citation: Tian, Fei, Jouha Min, Jiri Kanka, Xiangzhi Li, Paula T. Hammond, and Henry Du. "Lab-on-Fiber Optofluidic Platform for in Situ Monitoring of Drug Release from Therapeutic Eluting Polyelectrolyte Multilayers." Optics Express 23, no. 15 (July 24, 2015): 20132.

As Published: http://dx.doi.org/10.1364/oe.23.020132

Publisher: Optical Society of America

Persistent URL: http://hdl.handle.net/1721.1/102405

Version: Author's final manuscript: final author's manuscript post peer review, without publisher's formatting or copy editing

Lab-on-fiber optofluidic platform for in-situ monitoring of drug release from therapeutic eluting polyelectrolyte multilayers

Fei Tian, [1,*] Jouha Min,[2,3] Jiri Kanka,[4] Xiangzhi Li,[1] Paula T. Hammond, [2,3] and Henry Du[1]

[1]*Department of Chemical Engineering and Materials Science, Stevens Institute of Technology, Hoboken, NJ 07030, USA*
[2]*Department of Chemical Engineering, Massachusetts Institute of Technology, Cambridge, MA 02139, USA*
[3]*David H. Koch Institute for Integrative Cancer Research, Cambridge, MA 02139, USA*
[4]*Institute of Photonics and Electronics AS CR, v.v.i., Chaberska 57, Prague 8 18251, Czech Republic*

[*]*ftian1@stevens.edu*

Abstract: A lab-on-fiber (LOF) optofluidic platform that provides physiologically relevant microenvironment was developed by integrating a long period grating (LPG) coupled with high order cladding mode to achieve high index sensitivity and a liquid-tight capillary tube assembly as a microfluidic chamber for LPG to mimic physiologically relevant microenvironment. We demonstrate the utility of LOF for in-situ monitoring the construction of the [chitosan (CHI)/poly (acrylic acid) (PAA)/gentamicin sulfate (GS)/PAA]$_n$ multilayers at monolayer resolution as well as evaluating the rate of GS release at a flow rate of 0.127 mL/min at 37 °C in real time. We reveal that GS is released at a faster rate under the dynamic flow condition than in a static medium. Our findings underscore the importance of conducting drug release studies in physiologically relevant conditions.

OCIS codes: (050.2770) Gratings; (060.2370) Fiber optics sensors; (280.4788) Optical sensing and sensors; (310.0310) Thin films.

References and links

1. H. Craighead, "Future lab-on-a-chip technologies for integrating individual molecules," Nature **442** (7101), 387–393 (2006).
2. X. Fan and I. M. White, "Optofluidic microsystems for chemical and biological analysis," Nature Photon. **5** (10), 591-597 (2011).
3. D. Psaltis, S. R. Quake, and C. Yang, "Developing optofluidic technology through the fusion of microfluidics and optics," Nature **442** (7101), 381-386 (2006).
4. N. T. Huang, H. L. Zhang, M. T. Chung, J. H. Seo, and K. Kurabayashi, "Recent advancements in optofluidics-based single-cell analysis: optical on-chip cellular manipulation, treatment, and property detection," Lab Chip **14** (7), 1230-1245 (2014).
5. G. M. Whitesides, "The origins and the future of microfluidics," Nature **442** (7101), 368-373 (2006).
6. P. S. Dittrich and A. Manz, "Lab-on-a-chip: microfluidics in drug discovery," Nature Rev. Drug Discov. **5** (3), 210-218 (2006).
7. P. T. Hammond, "Engineering materials layer-by-layer: challenges and opportunities in multilayer assembly," AIChE J. **57** (11), 2928–2940 (2011).
8. J. Min, R. D. Braatz, and P. T. Hammond, "Tunable staged release of therapeutics from layer-by-layer coatings with clay interlayer barrier," Biomaterials **35** (8), 2507-2517 (2014).
9. G. Decher, "Fuzzy nanoassemblies: toward layered polymeric multicomposites," Science **277** (5330), 1232-1237 (1997).
10. A. N. Zelikin, "Drug releasing polymer thin films: new era of surface-mediated drug delivery," ACS Nano **4** (5), 2494-2509 (2010).
11. A. Vengsarkar, P. Lemaire, J. Judkins, V. Bhatia, and J. Sipe, "Long-period fiber-grating-based gain equalizers," Opt. Lett. **21** (5), 335-338 (1996).
12. T. Erdogan, "Fiber grating spectra," J. Lightwave Technol. **15** (8), 1277–1294 (1997).

13. F. Tian, J. Kanka, and H. Du, "Long-period grating and its cascaded counterpart in photonic crystal fiber for gas phase measurement," Opt. Express **20** (19), 20951-20961 (2012).
14. Z. He, F. Tian, Y. Zhu, N. Lavlinskaia, and H. Du, "Long period gratings in photonic crystal fiber as an optofluidic label-free biosensor," Biosens. Bioelectron. **26** (12), 4774-4778 (2011).
15. R. Garga, S. M. Tripathi, K. Thyagarajan, and W. J. Bock, "Long period fiber grating based temperature-compensated high performance sensor for bio-chemical sensing applications," Sensor. Actuat. B-Chem. **176**, 1121– 1127 (2013).
16. Z. Wang, J. R. Heflin, R. H. Stolen, and S. Ramachandran, "Highly sensitive optical response of optical fiber long period gratings to nanometer-thick ionic self-assembled multilayers," Appl. Phys. Lett. **86** (22), 223104 (2005).
17. F. Tian, Z. He, and H. Du, "Numerical and experimental investigation of long-period gratings in photonic crystal fiber for refractive index sensing of gas media," Opt. Lett. **37** (3), 380–382 (2012).
18. S. Korposh, S. W. James, S.-W. Lee1, S. Topliss, S. C. Cheung, W. J. Batty, and R. P. Tatam, "Fiber optic long period grating sensors with a nanoassembled mesoporous film of SiO_2 nanoparticles," Opt. Express **18** (12), 13227-13238 (2010).
19. R. Z. Yang, W. F. Dong, X. Meng, X. L. Zhang, Y. L. Sun, Y. W. Hao, J. C. Guo, W. Y. Zhang, Y. S. Yu, J. F. Song, Z. M. Qi, and H. B. Sun, "Nanoporous TiO_2/polyion thin-film-coated long-period grating sensors for the direct measurement of low-molecular-weight analytes," Langmuir **28** (23), 8814-8821 (2012).
20. J. Keith, L. C. Hess, W. U. Spendel, J. A. Cox, and G. E. Pacey, "The investigation of the behavior of a long period grating sensor with a copper sensitive coating fabricated by layer-by-layer electrostatic adsorption," Talanta **70** (4), 818-822 (2005).
21. F. Tian, J. Kanka, X. Li, and H. Du, "Monitoring layer-by-layer assembly of polyelectrolyte multi-layers using high-order cladding mode in long-period fiber gratings," Sensor. Actuat. B-Chem. **196**, 475-479 (2014).
22. S. D. Puckett and G. E. Pacey, "Detection of water in jet fuel using layer-by-layer thin film coated long period grating sensor," Talanta **78** (1), 300-304 (2009).
23. Cusano, A., Consales, M., Crescitelli, A., Ricciardi, A., *Lab-on-fiber technology* (Springer, 2015).
24. F. Tian, J. Kanka, B. Zou, K. S. Chiang, and H. Du, "Long-period gratings inscribed in photonic crystal fiber by symmetric CO2 laser irradiation," Opt. Express **21** (11), 13208-13218 (2013).
25. Eduardo Guzmán, Jesica A. Cavallo, Raquel Chuliá-Jordán, César Gómez, Miriam C. Strumia, Francisco Ortega, and Ramón G. Rubio, "pH-Induced changes in the fabrication of multilayers of poly(acrylic acid) and chitosan: fabrication, properties, and tests as a drug storage and delivery system," Langmuir **27** (11), 6836–6845 (2011).
26. Z. Sui, D. Salloum, and J. B. Schlenoff, "Effect of molecular weight on the construction of polyelectrolyte multilayers: stripping vs. sticking," Langmuir **19** (6), 2491-2495 (2003).
27. S. A. Sukhishvili, E. Kharlampieva, and V. Izumrudov, "Where polyelectrolyte multilayers and polyelectrolyte complexes meet," Macromolecules **39** (26), 8873–8881 (2006).
28. T. Nakano, J. R. Thompson, R. J. Christopherson, and F. X. Aherne, "Blood flow distribution in hind limb bones and joint cartilage from young growing pigs," Can. J. Vet. Res. **50** (1), 96–100 (1986).
29. JE. Jr. Fleming, C. N. Cornell, and G. F. Muschler, "Bone cells and matrices in orthopedic tissue engineering," Orthop. Clin. North. Am. **31** (3), 357-374(2000).
30. E. Truumees and H. N. Herkowitz. "Alternatives to autologous bone harvest in spine surgery," Univ. of Penn. Ortho. J. **12**, 77-88(1999).
31. J. S. Moskowitz, M. R. Blaisse, R. E. Samuel, H. P. Hsu, M. B. Harris, S. D. Martin, J. C. Lee, M. Spector, and P. T. Hammond, "The effectiveness of the controlled release of gentamicin from polyelectrolyte multilayers in the treatment of Staphylococcus aureus infection in a rabbit bone model," Biomaterials **31** (23), 6019-6030 (2010).
32. Eugenia Kharlampieva, John F. Ankner, Michael Rubinstein, and Svetlana A. Sukhishvili, "pH-induced release of polyanions from multilayer films," Phys. Rev. Lett. **100** (12), 128303 (2008).
33. B. Smitha, S. Sridhar, and A. A. Khan, "Polyelectrolyte Complexes of Chitosan and Poly(acrylic acid) As Proton Exchange Membranes for Fuel Cells," Macromolecules **37**, 2233-2239 (2004).

1. Introduction

Lab-on-a-Chip (LOC), a technology based on microfluidic devices lithographically fabricated on silicon, glass, and/or polymer with integrated capabilities of fluidic flow control and process (physical, chemical, or biological) monitoring, has proven robust utility for diverse applications ranging from chemical/biological measurements, cell sorting, drug discovery, and even 3D human tissue culture as in vitro model for drug screening and evaluation [1-4]. Benefits of the scaling laws due to rapid molecular transport, fast heat transfer, high surface-to-volume ratio for high throughput and high sensitivity in conjunction with the ability to mimic physiological microenvironment for human health research are the principal drivers for the thriving LOC of increasing complexity and expanding capabilities [5,6].

While highly attractive, LOC does not lend itself readily for exploration and exploitation of many significant systems in microenvironment. One such system is therapeutic-eluting polyelectrolyte coatings deposited via layer-by-layer (LbL) assembly for medical implants and tissue scaffolds intended for clinical care of patients, a frontier field of growing attention and impact [7-10]. Efficacy of the coating requires controlled and sustained release with dose profiles tailored to specific needs. As such, accurate knowledge on release kinetics and associated mechanisms is essential in the development and eventual clinical insertion of promising LbL therapeutic strategies. There are two significant challenges in employing LOC in drug-release study of the LbL systems. First, the coatings are typically microns in thickness for prolonged drug release and require hundreds and even thousands of repetitive LbL steps to deposit, making coating construction in a microfluidic channel unrealistic and cost-prohibitive. Second, on-chip interrogation using the common and highly sensitive fluorescence detection method would require labeling the drug with fluorescent molecules, which could change the release characteristics and/or alter the nature of the drug. Other techniques such as absorption spectroscopy, electrochemical methods, and mass spectrometry, either do not have the sensitivity or would add major systems integration complexity and cost for in-line integration.

Here, to overcome the above challenges and to advance the LbL frontier, we develop and optimize an innovative all-optical, lab-on-fiber (LOF) optofluidic platform for real-time, in-situ, and label-free measurements of the drug release processes of LbL coatings and demonstrate the utility of this LOF platform by studying the release profiles in physiologically relevant microenvironment with release in open buffer solution as control. The LOF platform consists of a single-mode optical fiber (SMF) with laser-inscribed long-period gratings (LPG) and a liquid-tight capillary tube assembly as a microfluidic chamber for SMF-LPG to mimic physiologically relevant microenvironment. LPG, periodic index perturbations typically hundreds of microns in periodicity, enables the coupling of the fundamental core mode ($LP_{0,1}$) to co-propagating cladding modes ($LP_{0,n}$,n = 2,3,4,…) in SMF at well-defined resonance wavelengths [11]. At a fundamental level, core mode $LP_{0,1}$ to cladding mode $LP_{0,n}$ coupling takes place when phase-matching condition, $\lambda_{resonance} = (n^{eff,\ core} - n^{eff,\ cladding})\Lambda$, is satisfied [12], where, $\lambda_{resonance}$ is the coupling resonance wavelength of the cladding mode, $n^{eff,\ core}$ and $n^{eff,\ cladding}$ are respective effective indices of the core and the cladding modes, and Λ is grating period. The dependence of $\lambda_{resonance}$ on $n^{eff,\ core}$ and $n^{eff,\ cladding}$ makes SMF-LPG an excellent candidate for sensitive index transduction platform [13-23]. Compared with other techniques such as absorption spectroscopy, electrochemical methods, and mass spectrometry, the LPG has both the sensitivity and ease for in-line systems integration for label free measurement.

A therapeutic-eluting LbL polymer model system [CHI/PAA/GS/PAA] is used for the demonstration of the robustness of the LOF optofluidic platform, where CHI, GS and PAA stand for chitosan, gentamicin sulfate and poly(acrylic acid), respectively. A capillary tube connected to a microflow pump was employed as a host for the LPG/LbL system to mimic physiologically relevant fluid flow in a microenvironment during drug release. Both the LbL growth of [CHI/PAA/GS/PAA] and the subsequent GS release was monitored by measuring the resonance wavelength change of the SMF-LPG using the most sensitive cladding mode in situ, which provides important insights into the LbL growth mechanism and drug release. Finally, the obtained experimental data were validated and correlated with the results obtained under conventional drug release conditions (i.e. static conditions using the radiolabel ^{3}H-GS). We show that the LOF optofluidic platform is robust and yields critical release information not readily available using static flow condition in a macro release medium. Such information is of vital importance in the development and clinical insertion of therapeutic-eluting polyelectrolyte films for patient care.

2. Fabrication of SMF-LPG

Numerical simulation is used to guide the mode selection and fabrication of SMF-LPG structures of the highest possible index sensitivity. For lower order cladding modes such as

$LP_{0,2}$ and $LP_{0,3}$, their index sensitivity is generally very low. On the other hand, higher order cladding modes give higher sensitivity due to a higher evanescent power overlap with the surrounding medium. A shorter periodicity is required for the coupling into a higher order of $LP_{0,10}$ cladding mode than that of the lower order of $LP_{0,2}$ cladding mode in the wavelength range of 1400~1700 nm. A SMF-LPG coupled with $LP_{0,10}$ cladding mode at grating periodicity predicted to exhibit response of higher sensitivity is fabricated.

A schematic of the fabrication setup is shown in Fig. 1(a). SMF-28 is used to inscribe LPG with the aid of 120º Au-coated Si reflection mirror by our CO_2 laser system to achieve SMF-LPG at grating periodicities predicted to exhibit the most sensitive response. The reflection mirror turns otherwise a unidirectional laser irradiation to an equivalent of three-beam process at incident angles 120º apart, thus enabling symmetrical LPG inscription. The CO_2 laser, equipped with a closed loop kit, has excellent power stability (< 1%), critical for fabricating reproducible LPG structure. The refractive index modulation arises from the so-called opto-elastic effect with its origin stemming from residual stress relaxation in SMF by rapid, localized laser heating without causing deformation. The laser is projected as a 3000 μm ×100 μm rectangular spot on SMF with the longer beam profile straddling the fiber in radial direction. The portion of SMF where LPG is inscribed is firmly mounted on a motorized, precision translation stage with 0.2 μm minimum incremental motion. The entire LPG structure is fabricated with laser irradiation and movement of the translation stage (thus LPG periodicity) controlled by computer interface. The transmission spectrum of the LPG is monitored in situ during the inscription process. LPG is inscribed in the SMF-28 at the period of 244.5 μm and length of 5.2 cm with the aid of 120º Au-coated Si reflection mirror by our CO_2 laser system [24]. A super-K ultra broadband supercontinuum light source and optical spectrum analyzer (OSA, Anritsu MS9710 C) is used to obtain the transmission spectrum during the SMF-LPG fabrication. The transmission spectrum of the as-fabricated SMF-LPG is shown in Fig. 1(b).

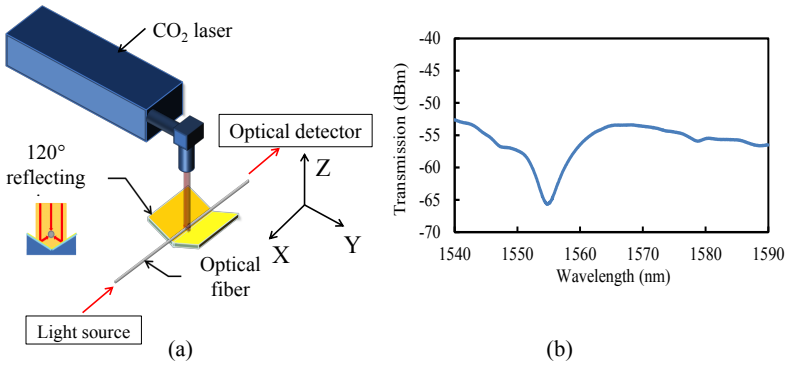

Fig. 1. (a) Schematic of the LPG fabrication setup; (b) transmission spectrum of the as-fabricated SMF-LPG.

3. Release characterization

For in-situ measurement, LPG loaded with LbL thin films was mounted in the center of a capillary tube with the inlet connected to the buffer supply and the outlet connected to a vial. It consists of two key components as illustrated in Fig. 2. One component is the SMF-LPG, the heart of the LOF platform. It plays two integral roles: as a substrate on which therapeutic-eluting LbL coatings can be deposited in open solution bath and as a fiber-optic sensor for in-situ measurements of drug release under physiologically relevant conditions via tracking the optical transmission in LPG. The other component is a liquid-tight capillary tube assembly as a microfluidic chamber for SMF-LPG to mimic physiologically relevant microenvironment. It

is configured with inlet and outlet for micro-pump flow regulation and submersible in a water bath for temperature control at human body temperature of ~37 °C. The two components, upon LbL deposition on SMF-LPG, are integrated to form LOF optofluidic platform for drug release evaluation. This LOF platform not only allows a continuous flow during the release process, but also enables the light coupling at the same time, hence constantly monitoring the shift of the resonance wavelength as the release process takes place. The phosphate buffer solution (PBS) at pH 7.4 was pressure pumped to the capillary tube and the pressure was chosen so that the flow rate of the PBS buffer solution was 0.127 mL/min. For radiolabel measurements, films with antibiotic GS (^{3}H-GS) were immersed into 1 mL of phosphate buffer solution (PBS) with pH 7.4 in a capped 2-mL microcentrifuge tube maintained at 37 °C. At predetermined time points, 0.5 mL of sample was collected from the tube and replaced with 0.5 mL of pre-warmed PBS. Details can be found in [8].

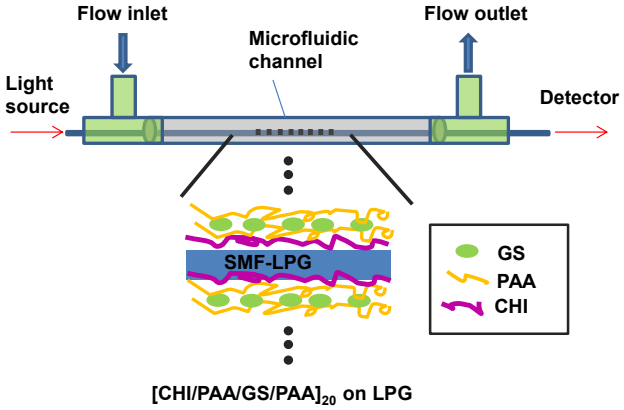

Fig. 2. Schematic of the LOF optofluidic platform submersible in heated water bath for drug release investigation. A microflow pump allows for continuous flow of buffer solution in the capillary tube whereas the all-optic interconnections make it possible for real-time, in-situ measurements of the drug release from the LbL coating deposited on the SMF-LPG platform.

4. LbL deposition of polyelectrolyte multilayers as monitored by SMF-LPG

Poly(acrylic acid) (PAA, Mw ~ 450 kDa), Chitosan (Chi, Mv ~ 60-120 kDa), 3 M sodium acetate buffer (NaOAc, pH 5.2), as well as solvents and common buffers, were purchased from SigmaeAldrich (St. Louis, MO). Dipping solutions of CHI and PAA were prepared at 2 mg/mL in 100 mM sodium acetate buffer and pH adjusted to 5.0. The dipping solution of GS was at 10 mg/mL in 100 mM sodium acetate buffer. Silicon substrates with dimensions of 0.5×2.0 cm^2 were used for static experiments. The substrate of SMF-28 with a length of 5.2 cm was fastened straight with two holders on a stage. It was dipped into a container with a V-groove holding the polymer solutions during the LbL deposition until the desired number of tetralayer was achieved on the SMF-28 platform. Tetralayer films were fabricated at room temperature by alternate dipping in a solution of cationic species for 5-6 min followed by two consecutive rinse steps in 100 mM sodium acetate baths for 1.5-2 min, and then into anionic species for 5-6 min followed by the same rinse cycle. The entire cycle was repeated until the desired number of tetralayers was deposited. The transmission spectra of SMF-LPG were obtained during the course of deposition to monitor the LbL growth.

The SMF-LPG coupled with $LP_{0,10}$ cladding mode [21] with a much higher sensitivity compared with that of lower order of cladding mode is fabricated and used for the LOF platform. Taking advantage of the sensitive nature of the SMF-LPG to the deposition of individual polyelectrolyte layers, we carried out LbL growth of $[CHI/PAA/GS/PAA]_n$ on SMF-LPG while measuring the resonance wavelength response in situ. The robustness of the SMF-LPG with $LP_{0,10}$ cladding mode to monitor the LbL deposition of a

$[CHI/PAA/GS/PAA]_3$ coating is shown in Fig. 3, where the resonance band in the light transmission through SMF-LPG is tracked by an OSA following successive deposition of each tetralayer building unit. Here, the SMF-LPG functions both as a coating substrate and a sensing platform. The large shift of ~2.7 nm per tetralayer of polyelectrolyte molecules deposited (OSA resolution: 0.05 nm) is a powerful indication of the promising nature of SMF-LPG for drug release measurements.

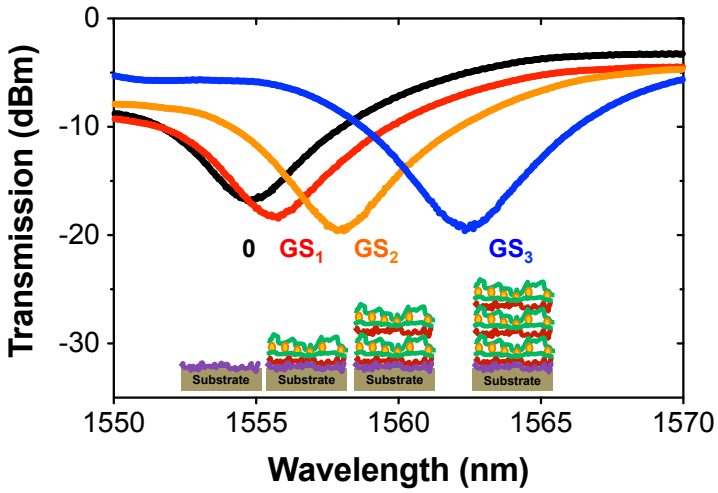

Fig. 3. Transmission spectra in SMF-LPG with the number of $[CHI/PAA/GS/PAA]_n$ (n=1,2,3) polyelectrolyte tetralayers as a parameter. Measurements were carried out in situ during the LbL process.

The SMF-LPG was further utilized to monitor, in situ, the individual adsorption events during LbL of 20 [CHI/PAA/GS/PAA] tetralayers or 80 total polyelectrolyte layers. Plotted in Fig. 4 is the shift in the resonance wavelength of the $LP_{0,10}$ mode as a function of the layer number as LbL took place for the first 7 tetralayers. Generally speaking, there is a red shift with the increase of the number of tetralayers deposited, indicating an overall increase in the thickness as the polyelectrolyte multilayers (PEM) are deposited on the LPG. The response of SMF-LPG to the deposition of the tetralayers shows a non-linear growth. Similar trend was observed for other multilayer assembly containing [CHI/PAA] deposited at pH 5 by Guzmán et al. [25]. This figure also shows that starting from the second tetralayer, for the deposition of the fourth layer (PAA (4th)) within each tetralayer unit, there is always a blue shift, indicating a decrease in the thickness of the thin film. This means in the current deposition condition, when the polyelectrolyte multilayer (PEM) is brought in contact with the polyelectrolyte solution for the fourth layer of PAA, slight contraction of the multilayers can occur. This is confirmed by the ellipsometry measurement of the thickness of the $[CHI/PAA/GS/PAA]_n$ thin films with GS and PAA (4th) as the terminal layer for the 1st through the 5th tetralayers, respectively. For the ellipsometry experiments, we have used home-built phase-modulated ellipsometer, and all of the experiments have been carried out on a solid liquid cell at a fixed angle of 70°. Silicon wafers were used as the substrates. Ellipsometry angles Δ and Ψ describe the changes in the state of polarization when light is reflected at a surface. A He–Ne laser of 2 mW power (JDS Uniphase) is used as a light source. Shown in Fig. 5 is the ellipsometry measurement of the thickness when the thin film is immersed in buffer solution the same as that for the thin film deposition. It shows that as the layer number increases, there is an increase in the thickness when taking the tetralayer as a unit. But within each tetralayer, the thickness of the thin film with GS as a terminal layer is always greater than that of the thin

film with PAA (4th) as the terminal layer. In another word, subsequent deposition of PAA on GS consistently results in some thickness reduction.

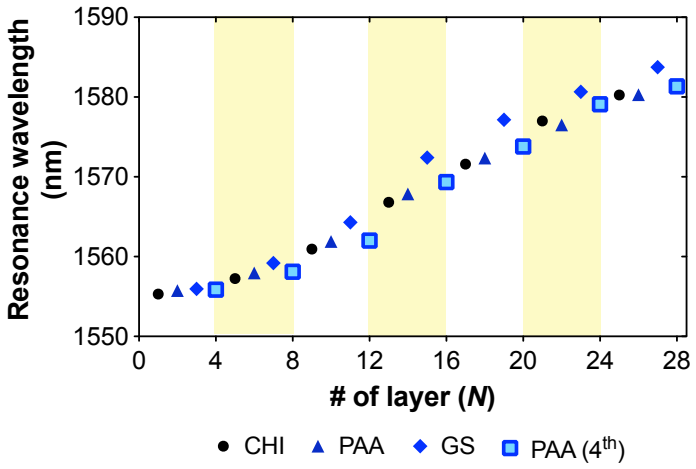

Fig. 4. Resonance wavelength of the coupled $LP_{0,10}$ cladding mode as a function of the number of [CHI/PAA/GS/PAA] layers deposited on LPG. Measurements were carried out in situ during LbL growth.

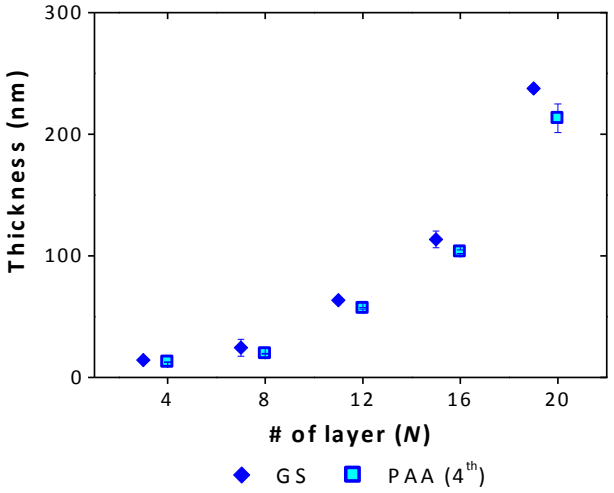

Fig. 5. Thicknesses of polyelectrolyte multilayers with GS and PAA (4th) as respective terminal layers. Data were obtained for the 1st through the 5th tetralayers in buffer solution at pH 5.

To take a close examination of the kinetics of the polyelectrolyte adsorption, the response of the SMF-LPG to the deposition of each of the constituent layers in a tetralayer unit with respect to deposition time is depicted in Fig. 6. It shows that for the deposition of the first three layers of CHI, PAA and GS, the coating thickness increases steadily (red shift), reaching a plateau within the first three minutes. Whereas during deposition of PAA in the fourth layer, the coating thickness decreases (blue shift), stabilizing only after an extended time period. Note that for polyelectrolyte systems in which chain exchange occurs at the experimental time scale, the excess of charged chains in bulk solution is most favorable for the formation of water-soluble polyelectrolyte complexes. When a polyelectrolyte chain is included within

such complexes, there is a gain in the translational and configurational entropy as well as a greater mobility of dissolved polyelectrolyte chains [26]. This is similar to the phenomenon that the balance between multilayer growth and polyelectrolyte chain removal is kinetically controlled, where there is initial accumulation of poly(methacrylic acid) (PMAA) at the surface and then followed by overwhelming removal of the water-soluble complexes [26, 27]. We note that the resonance wavelength at the initial of PAA deposition is larger than that of the plateau of the CHI deposition. Throughout the deposition process of CHI, the response is measured upon immersion of the LPG in the CHI solution till completion of the deposition as reflected by the stable resonance wavelength. The same can be said for PAA and GS depositions but in their respective solutions of different indices of refraction. The significantly higher GS solution concentration (10 mg/mL) and hence higher index of refraction, as compared to that of the PAA solution (2 mg/mL), can be attributed to the large red shift in the resonance wavelength during GS deposition. At the meantime, the deposition of PAA takes place instantly after we immerse the LPG in the PAA solution whereas the data acquisition takes about 10 seconds to complete. The first measured resonance wavelength reflects actually a situation where PAA layer has already been formed, thus an appreciable red shift at the beginning of the deposition process, compared to the plateau of the CHI deposition.

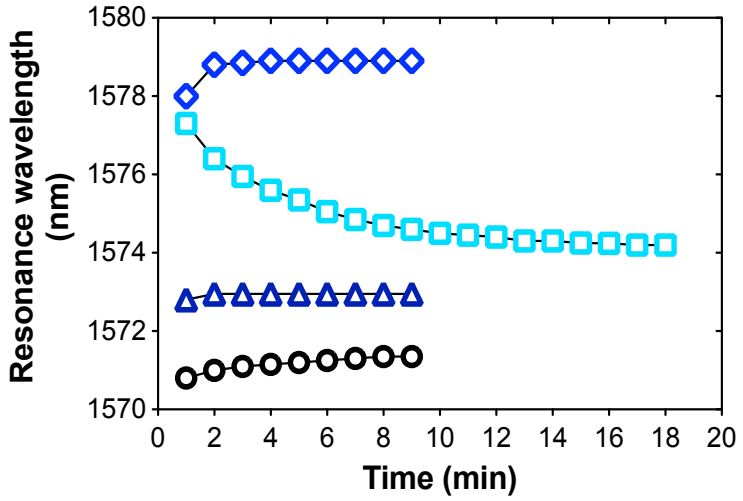

Fig. 6. Time-resolved monitoring of monolayer deposition for the respective CHI, PAA, GS and PAA (4th) layers within a tetralayer unit.

5. In-situ measurements of the release profiles using LOF optofluidic platform

Optimal drug dosage and release profiles under physiologically relevant conditions are essential for the development of drug-delivery implants for patient care. These conditions can only be established by means of monitoring the release profiles under dynamic conditions in real time. SMF-LPG coated with $[CHI/PAA/GS/PAA]_{20}$ is integrated with the LOF optofluidic platform (Fig. 2) for in-situ GS release measurements under physiologically relevant flow conditions in microenvironment. The highly sensitive SMF-LPG allows us to monitor the shift in resonance wavelength as GS release and associated changes taking place. Our facile yet robust capillary tube-based host configuration aided by a microflow pump gives us the feasibility to work with a range of microchannel diameters (i.e., inner diameter of commercial capillary tube) as well as fluid flow rate. We examine the release profiles using capillary tubes of 1160 μm in inner diameter (D) at flow rates of 0.127 mL/min. Fresh PBS at pH=7.4 was pumped through the capillary tube at a flow rate of 0.127 mL/min, which is in the

range of blood flow calculated for cancellous bone and cortical bone of 20-week-old pigs [28]. In consideration of the diameter of coated SMF-LPG (125 μm for SMF-LPG plus twice the coating thickness (2T) in wet stage), the fluid flow space in a fully assembled optofluidic platform is ½(D-125-2T). Using this formula and assuming a wet thickness of 15 μm per 10 tetralayers (n=10), the flow space (d) for the chosen capillary tube diameters and the coatings is 487.5 μm, which is in physiologically relevant range. For example, the commonly used osteoconductive scaffolds for bone graft have pore diameters ranging from 100 to 500 μm [29, 30]. Fig. 7 depicts time-dependent shift in the resonance wavelength of broad-band light transmission in SMF-LPG with an initial $[CHI/PAA/GS/PAA]_{20}$ coating in the LOF platform. Spectra were first recorded every 1 minute for the first 30 minutes due to initial rapid release, followed by every 2 hours up to 48 hours due to steady and slower release. The release of the GS tends to decrease the thickness of the thin film, which in turn decreases the effective refractive index of the surrounding of SMF-LPG, resulting in a blue shift in the transmission spectra.

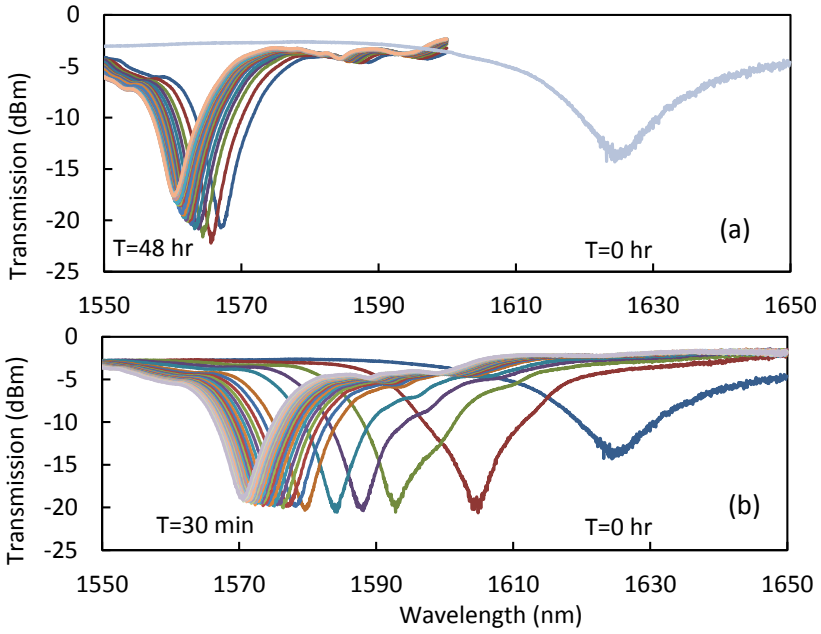

Fig. 7. Drug release measurement of SMF-LPG coated with $[CHI/PAA/GS/PAA]_{20}$ using the LOF optofluidic platform with time as parameter: (a) transmission spectra recorded every 30 mins up to 48 hours; (b)transmission spectra recorded every 1 minute in the first half an hour.Time-resolved monitoring of monolayer deposition for the respective CHI, PAA, GS and PAA (4th) layers within a tetralayer unit.

The release profiles of the $[CHI/PAA/GS/PAA]_{20}$ under dynamic flow condition obtained by the LOF and static condition in a test tube obtained by the radiolabel method are compared in Fig. 8. In both cases, GS begins to release immediately upon immersion with an initial burst drug elution, followed by a prolonged release at a much slower rate. Overall, the first burst release is due to the excess amount of GS diffusion out from the thin film, reduction of the charge state of GS by the increase of the pH from 5 to 7.4, and the salts of the PBS buffer diffuse into the thin film to compete with the ionic sites of GS [31]. As a result, PAA also releases from the thin film as a tail of GS release. Meanwhile, the pH-induced imbalance of negative to positive charges in the film is the driving force for PAA molecules to diffuse out of the thin film due to the so called “sticky gel electrophoresis” similar to that of PMAA: when negative charges accumulate within the film, PMAA chains with excess charge are

released into solution to bring the ratio of '-' to '+' polymer charges back to its original value close to unity [32].

The experimental studies under dynamic and static conditions revealed significant differences in the release profiles, however. During the burst release stage, within the first hour, more than 50% drug was released in dynamic flow using LOF platform. In contrast, it took about 5 hours to reach a similar level of release under static condition. Overall, the polyelectrolyte multilayers exhibited a much faster release profile under dynamic flow condition than under static condition. Under continuous flow of fresh PBS, a high concentration gradient is maintained, which acts as a driving force for rapid drug. Release process under dynamic flow reached the plateau in about 12 hours, whereas it underwent a much longer process under static condition, as evident by the still ongoing release after 48 hours shown in Fig. 8 red curve.

The release process of our drug-eluting system is predominantly diffusion-controlled, as confirmed in our modeling of the release profiles. The CHI and PAA are well documented in the study of the formation of proton exchange membranes for fuel cells. After the release of GS from the thin film, there is strong ionic interactions between CHI and PAA including (i) ionic cross-linking between ammonium ion (NH^{3+}) of CHI and carboxylateion (COO^-) of PAA, (ii) hydrogen bonding between $H^+$of carboxylic group of PAA and OH^- of CHI, and (iii) hydrogen bonding between H^+ of CHI and OH^- of carboxylic group of PAA. These complex interactions ensure adequate thermal and mechanical stability of the blend of CHI and PAA as demonstrated in an early report [33]. Taken as a whole, the initial drug burst release is due predominantly to large concentration gradient between the drug-eluting coating and the flowing medium. On the other hand, during the initial release process, it is possible that the polymer matrix is vulnerable due to the mismatch of the ionic interactions when the GS diffuses out of the polymer matrix. The flow-induced shear at the multilayer-medium interface is thus likely another factor that promotes rapid release as well as desorption of polyelectrolyte layers. We note that the actual amount of GS released to the PBS in the LOF platform needs to be determined to establish a calibration curve to correlate the shift of resonance wavelength with the release dosage. It can be accomplished by collecting the eluting solutions for radiolabel ^{3}H-GS quantification. We intend to carry out this investigation as part of a planned future study.

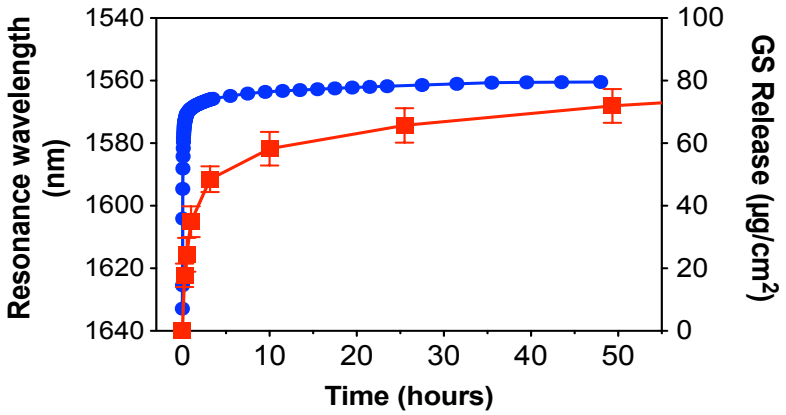

Fig. 8. Release profiles of $[CHI/PAA/GS/PAA]_{20}$ in (a) LOF under dynamic flow of phosphate buffered saline (PBS) solution as represented by the time-dependence shift in the resonance wavelength and (b) the GS release profile of $[CHI/PAA/GS/PAA]_{20}$ on silicon substrate in static open PBS buffer solution as measured by the well-established [^{3}H] radiolabel method.

6. Conclusion

We have developed a LOF optofluidic platform for the monitoring of the construction and release of LbL drug delivery polyelectrolyte multilayers under physiologically relevant

microenvironment. Our approach, first to the best of our knowledge, offers an exciting new opportunity to investigate LbL therapeutic release at monolayer precision under physiologically relevant conditions. It has as its core a LPG structure coupled with $LP_{0,10}$ cladding mode highly sensitive at individual layer level which is integrated with a capillary tube to mimic physiologically relevant microenvironment for in-situ and label-free measurements of release kinetics. The LOF platform has enabled the measurements of the release profiles of GS in-situ with fluid flow and flow spacing in the physiologically relevant ranges. Our results show that continuous flow of fresh medium allows the maintenance of a higher concentration gradient and thus leads to more rapid release, compared to static condition, for a diffusion-dominated process. In addition, dynamic flow inevitably introduces shear stress and hence potentially accelerates release for an erosion-controlled process. These results show that the LOF platform provide rich information and enables the in situ and real time study of the drug release process, which is more accurate than those obtained using conventional static method. The LOF optofluidic platform has the potential as a test bed for the determination of the kinetics and mechanisms of drug release in physiologically relevant microenvironment, critical for therapeutic-eluting coating design and development.

Acknowledgments

This work was sponsored by the US National Science Foundation under grant number DMR-1206669 and by the Ministry of Education, Youth and Sport of the Czech Republic under grant number LH 11038 within the U.S.-Czech S&T Cooperation agreement. We are indebted to Prof. Svetlana A. Sukhishvili for her insightful comments and suggestions for the work conducted.